

## Supporting Information

### Creating a synthetic platform for the encapsulation of nanocrystals with covalently bound polymer shells

Rieke Koll,<sup>‡,a</sup> Lisa Sarah Fruhner,<sup>‡,b,c</sup> Hauke Heller,<sup>a</sup> Jürgen Allgaier,<sup>b</sup> Wim Pyckhout-Hintzen,<sup>b</sup> Margarita Kruteva,<sup>\*,b</sup> Artem Feoktystov,<sup>d</sup> Ralf Biehl,<sup>b</sup> Stephan Förster<sup>b,c</sup> and Horst Weller<sup>\*,a</sup>

- a. Institute of Physical Chemistry, Grindelallee 117, 20146 Hamburg, Germany
- b. Jülich Centre for Neutron Science (JCNS-1) and Institute of Complex Systems (ICS-1), Forschungszentrum Jülich GmbH, Leo-Brandt-Straße, 52425 Jülich, Germany
- c. Institute of Physical Chemistry, RWTH Aachen University, Landoltweg 2, 52056 Aachen, Germany
- d. Forschungszentrum Jülich GmbH, Jülich Centre for Neutron Science (JCNS) at MLZ, Lichtenbergstrasse 1, 85748 Garching, Germany

#### Polymer synthesis

**General procedures.** All manipulations were carried out at a high vacuum line or in a glove box filled with Argon (M Braun, Unilab). The water level in the glove box was below 1 ppm and the oxygen level below 0.1 ppm. The flasks for all manipulations were equipped with Teflon stopcocks (Young® or Gebr. Rettberg GmbH), which allowed the transfer of materials between the vacuum line and glove box without contamination with air. The flasks that were exposed to overpressure were pressure-tested to 4-12 bar depending on the size of the flask.

**Materials.** Butadiene (Aldrich,  $\geq 99.6\%$ ) was degassed, condensed on solvent free di-*n*-butylmagnesium, stirred at RT overnight, condensed on solvent free *n*-butyllithium, stirred at  $-20\text{ }^{\circ}\text{C}$  for 20 min and directly used by condensing the monomer into the polymerization flask. Ethylene oxide (EO) (Chemogas,  $\geq 99.9\%$ ) was condensed into a flask, degassed and stirred twice over  $\text{CaH}_2$  for 1-2 days, before being condensed into the reaction flask. THF (VWR,  $\geq 99.5\%$ ) was degassed and dried with potassium and benzophenone before use. Dimethyl chlorophosphate (Sigma-Aldrich, 96%) was filled into a flask and degassed to remove traces of hydrogen chloride before use. Iodomethane (Sigma-Aldrich,  $>99\%$ ) was degassed and dried by stirring over  $\text{CaH}_2$  before use. Diethylen glycol monomethyl ether (Sigma-Aldrich, 99.5%) was degassed before use. Methanol (VWR,  $\geq 99.8\%$ ), dichloromethane (Sigma-Aldrich,  $\geq 99.9\%$ ), ethyl acetate (Sigma-Aldrich,  $\geq 99.7\%$ ), 1-methyl-2-pyrrolidone (Sigma-Aldrich, 99.5%), sodium bromide (AlfaAesar,  $\geq 99.5\%$ ), trimethylsilyl chloride (Fluka,  $\geq 99.0\%$ ), potassium *tert*-butoxide (Sigma-Aldrich 99.9%) diethyl vinylphosphonate (Sigma-Aldrich, 97%), potassium (Acros Organics,  $\geq 98\%$ ) and DMF (Sigma-Aldrich, 99.8%) were used as received.

**Polymerization reactions.** The synthesis of polybutadiene end functionalized with an OH-group (PB-OH) and PB-DETA is described elsewhere.<sup>1</sup> For the largest PB block with a molecular weight of about 4750 g/mol the synthesis procedure was changed slightly so that the polymerization took place at  $-60\text{ }^{\circ}\text{C}$  for the whole time and the ethylene oxide was distilled into the flask at  $-60\text{ }^{\circ}\text{C}$  instead of  $0^{\circ}\text{C}$  leading to an almost quantitative functionalization of the polymer end. For the largest block copolymer the synthesis procedure was also slightly changed to replace ethanol by acetone during the purification process. The block copolymer PB2k-*b*-dPEO5k was synthesized as described elsewhere<sup>1</sup> by replacing hydrogenous ethylene oxide (h-EO) by deuterated ethylene oxide (d-EO, Cambridge Isotope Laboratories, deuteration degree 98%).

Two methods were tried to obtain 1,2-polybutadiene end functionalized with a phosphonic acid group (PB2k-PA and PB5k-PA).<sup>2</sup>

1) 1,2-Polybutadiene was obtained by polymerizing 8.45 g of butadiene with 4.2 mmol of sec-butyllithium in 50 ml of THF at  $-60\text{ }^{\circ}\text{C}$  for 2 h. Afterwards, 3.03 g of dimethyl chlorophosphate was added under Argon and the reaction mixture was allowed to warm up to room temperature over-night leading to the precipitation of a white solid which dissolved upon the addition of 2 ml of methanol. After stirring for 5 min, the solvent was partially removed by vacuum distillation. The polymer was precipitated in methanol, washed with

methanol and dried under vacuum conditions. NMR analysis revealed incomplete functionalization of the polymer. To separate the polymer fraction with phosphonate end group, the product was purified via column chromatography using first dichloromethane to elute the non-functionalized polymer (70 %) and afterwards a 1:1 mixture of ethyl acetate and methanol for the functionalized polymer (26 %). The latter was washed three times with methanol and dried in vacuum. To cleave the ester groups, the functionalized polymer was dissolved in 20 ml of 1-methyl-2-pyrrolidone. Upon addition of 0.295 g of sodium bromide and 400  $\mu$ l of trimethylsilyl chloride, the solution was stirred for 17 h at 50 °C. After removal of the solvent by vacuum distillation, the polymer was washed two times with methanol and dried under high vacuum conditions. The purity of the functionalized product was checked via thin-layer chromatography (TLC).

2) 1.038 g (0.2 mmol) of 1,2-polybutadiene end functionalized with an OH-group ( $M = 5000$  g/mol) was added to a Schlenk flask and degassed under high vacuum conditions. In a glovebox, 0.0248 g potassium *tert*-butoxide (0.2 mmol) was dissolved in dry THF and added to the flask. After stirring for 3 h, solvent and formed *tert*-butanol were removed under high vacuum conditions. 30 ml of THF, 10 ml of DMF and 0.3625 g (2.2 mmol) of diethyl vinylphosphonate were added to the flask in a glovebox. The reaction was terminated after 27 h by removal of the solvent under high vacuum conditions. The ester hydrolysis and purification steps were the same as described in 1). The full functionalization of the polymer was confirmed by the absence of the signal for the  $\text{CH}_2\text{-OH}$  protons in the  $^1\text{H}$  NMR spectrum of the product in deuterated pyridine.

The PEO homopolymers PEO3k and dPEO3k were synthesized from h-EO and d-EO using the techniques described elsewhere.<sup>1</sup> The potassium salt of diethylene glycol monomethyl ether (KDGME) was used as initiator and dry toluene as solvent. The mass fraction of EO in the toluene/EO mixture was about 10% and the reaction temperature was increased from 35 °C to 55 °C over two days and kept at 55 °C for another 3 days. The polymerization reactions were terminated with a tenfold excess of dry hydrogenous iodomethane. After four hours the excess of iodomethane and the solvent were removed by vacuum distillation. The raw products were dissolved in chloroform, washed with water and after removal of most of the solvent precipitated in heptane. The products were finally dried under vacuum conditions. KDGME was synthesized by reacting potassium metal with a small excess of diethylene glycol monomethyl ether in a triple amount of dry toluene. After the disappearance of the

potassium, the solvent was distilled off and the excess of the alcohol was removed under high vacuum conditions at 80 °C.

dPEO10k was synthesized using triethylene glycol as initiator, metalated to 15% with potassium. Dry THF was the solvent. The polymerization was carried out in a metal reactor at 100 °C overnight. The reaction was terminated with acetic acid. The purification steps are the same as for the PEO3k.

### **Polymer characterization**

The molecular weight distributions  $M_w/M_n$  of samples 1,2-PB-OH and 1,2-PB-*b*-PEO were determined by size exclusion chromatography (SEC) using a SEC instrument consisting of Agilent 1260 Infinity pump (G1310B) and autosampler (G1329B), three Agilent PlusPore GPC columns with a continuous pore size distribution, a Shimadzu CTO-20AC column oven and a differential refractive index (Wyatt Optilab T-rEX) as well as a light scattering detector (Wyatt DAWN Heleos-2). The eluent was a mixture of THF and DMA (85:15 by volume) at a flow rate of 1 mL/min at 50 °C. The data were evaluated using ASTRA6.1 software, determining the refractive index increment from the polymer peak and calculating the absolute molecular weights from the light scattering signal. The molecular weight characterization of the PB-DETA and PB-PA samples were carried out with the polymers prior to the functionalization reaction due to the absorption of the functionalized polymers on the SEC columns.

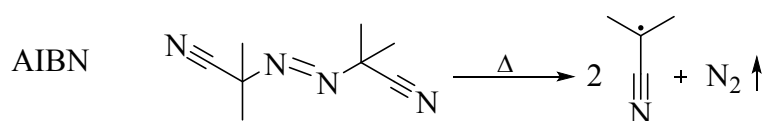
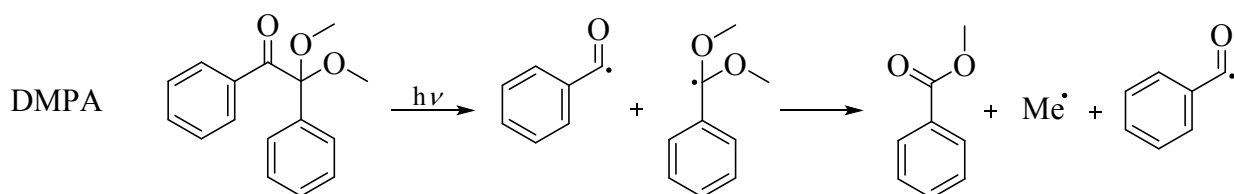
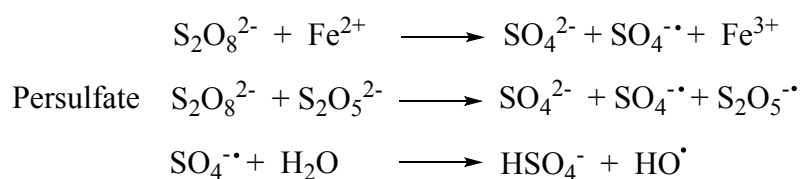
The microstructure of the PB block as well as the functionalization of the polymer ligands were defined via <sup>1</sup>H-NMR as described elsewhere.<sup>1</sup>

**Table 1S:** Molecular weight characterization of the polymers used for the SPION encapsulation processes.

<b>polymer</b>	<b><math>M_n</math> (g/mol)</b>	<b><math>M_w/M_n</math></b>
PB2k-dPEO5k	6580	1.02
PB2k-PEO5k	6790	1.02
PB3k-PEO4k	7710	1.00
PB5k-PEO10k	14800	1.01
PB2k-DETA	1920	1.02
PB3k-DETA	2930	1.01
PB2k-PA	2180	1.03
PB5k-PA	4750	1.00
PEO3k*	3020	1.04
dPEO3k*	2940	1.03
dPEO10k*	10500	1.03
PEO3k (Sigma Aldrich)	3370	1.03
PEO10k (Sigma Aldrich)	10400	1.06

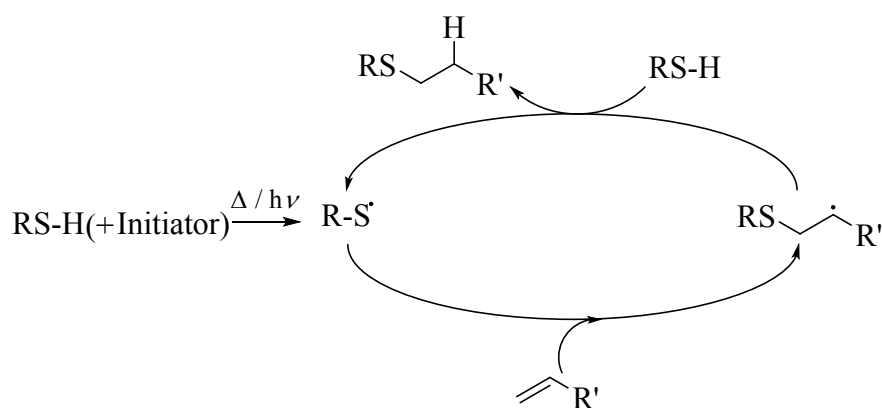
\* These data were evaluated using a standard calibration for PEO

### Crosslinking reactions

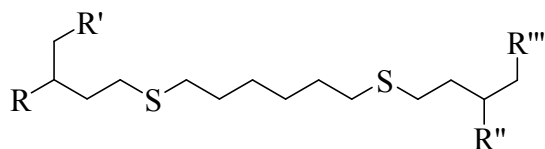


**Scheme 1S:** Decomposition reactions of the used initiators to start the crosslinking process.<sup>3-6</sup>

The crosslinking of polydienes is well-known, information on the mechanism can be found in the literature.<sup>7,8</sup>



**Scheme 2S:** Reaction mechanism of the thiol-ene clickreaction.<sup>9</sup>



**Scheme 3S:** Polymer structure after crosslinking with HDT as crosslinker.

### TEM of differently crosslinked samples

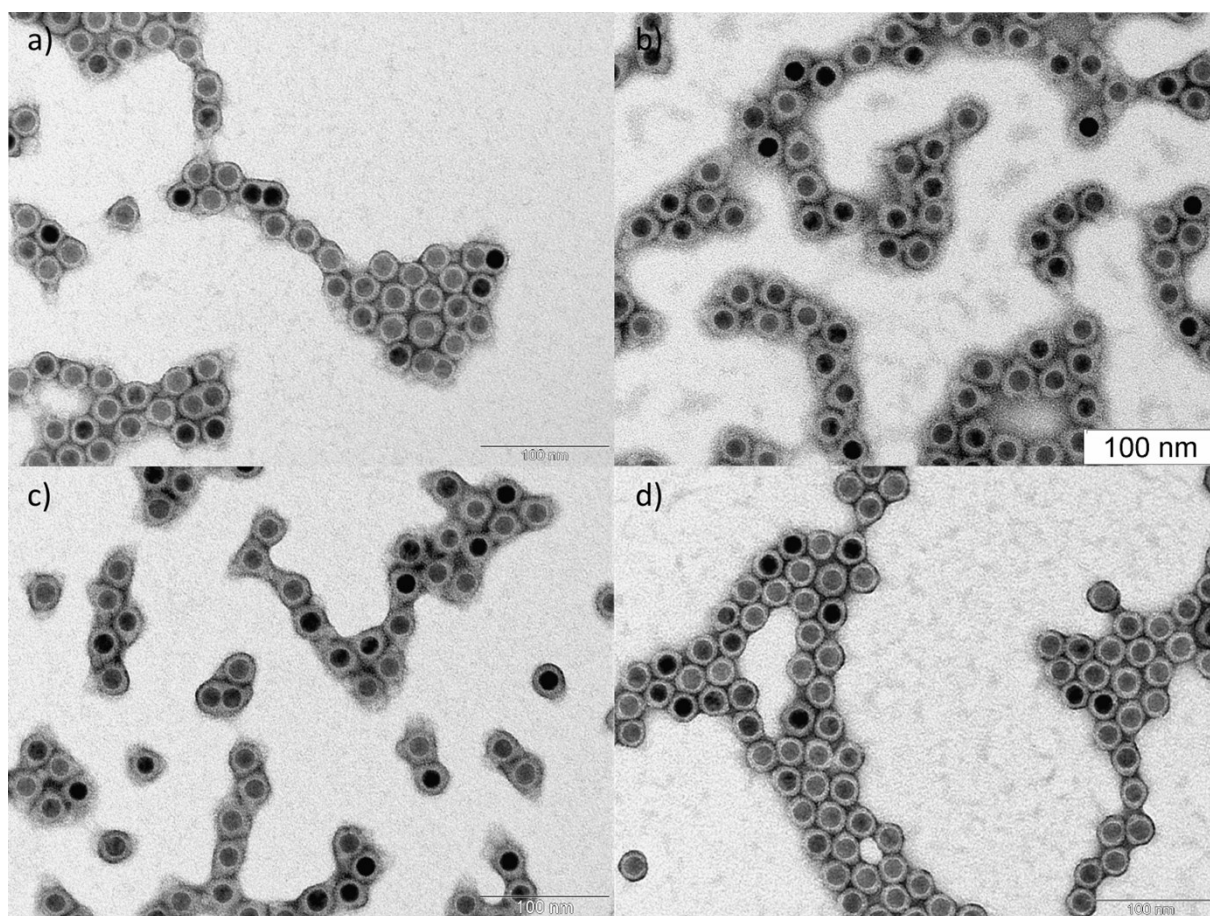


**Figure 1S:** TEM images of HDT/AIBN (a) HDT/UV (b) HDT/DMPA/UV (c) and persulfate (d) crosslinked encapsulated SPIONs, stained with phosphotungstic acid. The diblock copolymers PB5k-PEO10k (b, c) and PB3k-PEO4k (a, d) were used.

### TEM images of phosphotungstic acid and osmium tetroxide stained polymer shells

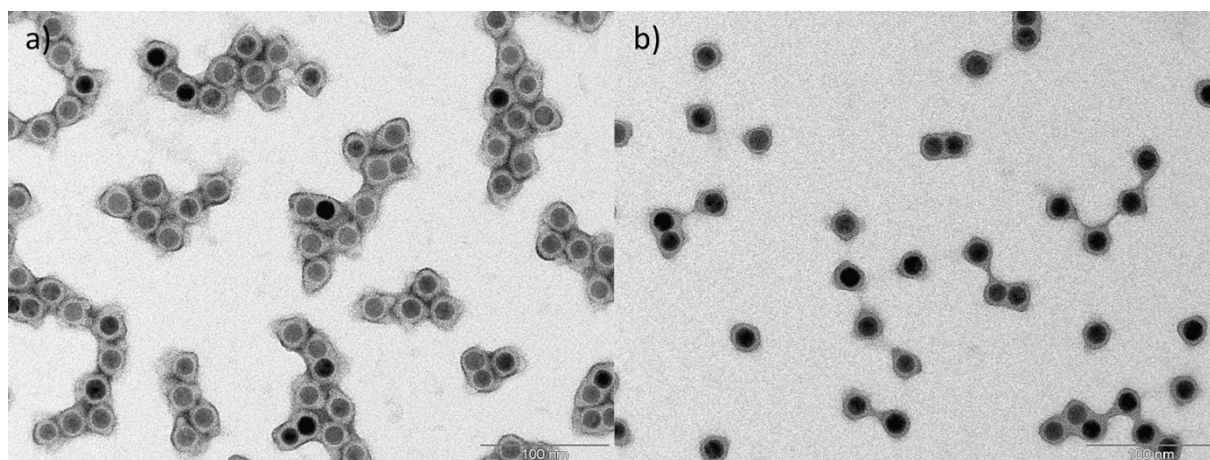


**Figure 2S:** TEM images of encapsulated SPIONs with phosphotungstic acid (a) and osmium tetroxide (b) stained polymer shells. The polymer shell consists of PB3k-PEO4k and was crosslinked with HDT/AIBN.

## TGA and DLS measurements of samples with different diblock copolymer sizes

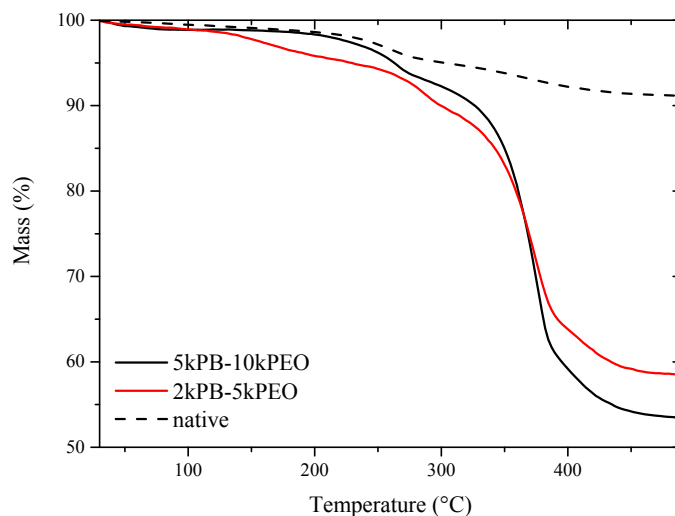


**Figure 3S:** Exemplary TGA results for PB2k-PEO5k and PB5k-PEO10k encapsulated SPIONs, crosslinked with HDT/AIBN, and TGA results for oleic acid stabilized SPIONs for comparison. The replacement of the oleic acid by the polymeric ligand was omitted to ensure that the organic compound mostly consists of the diblock copolymer. The diblock copolymer and NC mass fractions were calculated from the relative mass losses between 100 °C and 450 °C and the residual mass at 450 °C, whereat a mass loss of 9% for oleic acid was subtracted. Considering the masses of the diblock chains and the NCs, the number of polymer chains per NC was calculated to be 230 chains for PB5k-PEO10k coated NCs and 360 chains for the PB2k-PEO5k coated NCs.

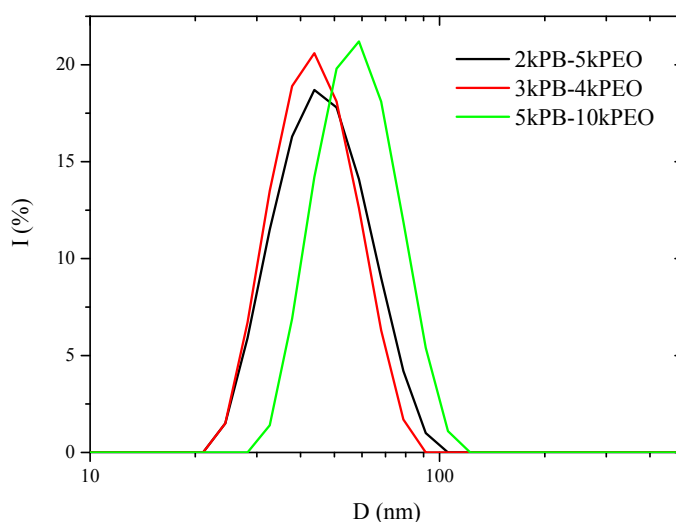


**Figure 4S:** Intensity weighted size distributions from DLS analysis for SPIONs encapsulated with different weighted diblock copolymers.

## SANS fit model

Our extended pearl-necklace model consists of a spherical core-shell-shell form factor  $P(Q)$  and an intra-agglomerate structure factor  $S_{intra}(Q)$ :

$$I(Q) \cong P(Q) \cdot S_{intra}(Q)$$

The form factor contains contributions from the core and both shells:

$$P(Q) = \left[ \frac{4\pi}{3}(\rho_c - \rho_m) \cdot R_c^3 \cdot A_1 + \frac{4\pi}{3}(\rho_{PB} - \rho_m) \cdot (R_c + t_{PB})^3 \cdot A_2 + \frac{4\pi}{3}(\rho_{PEO} - \rho_m) \cdot R^3 \cdot A_3 \right]^2$$

$$A_1 = 3 \frac{\sin(QR_c) - QR_c \cdot \cos(QR_c)}{(QR_c)^3}$$

$$A_2 = 3 \frac{(\sin(Q(R_c + t_{PB})) - Q(R_c + t_{PB}) \cdot \cos(Q(R_c + t_{PB}))) - (\sin(QR_c) - QR_c \cdot \cos(QR_c))}{(Q(R_c + t_{PB}))^3 - (QR_c)^3}$$

$$A_3 = 3 \frac{(\sin(QR) - QR \cdot \cos(QR)) - (\sin(Q(R_c + t_{PB})) - Q(R_c + t_{PB}) \cdot \cos(Q(R_c + t_{PB})))}{QR^3 - Q(R_c + t_{PB})^3}$$

$$R = R_c + t_{PB} + t_{PEO}$$

The structure factor is the same as in the original model:

$$S_{intra}(Q) = \frac{2}{N^2} \left[ \frac{N}{1 - \frac{\sin(Q(l+2R))}{Q(l+2R)}} - \frac{N}{2} - \frac{1 - \left( \frac{\sin(Q(l+2R))}{Q(l+2R)} \right)^N \sin(Q(l+2R))}{\left( 1 - \frac{\sin(Q(l+2R))}{Q(l+2R)} \right)^2 Q(l+2R)} \right]$$

## SANS fit results

**Table 2S:** Fit parameters for SANS data. Highlighted in grey are the fixed values for the fits,  $R_c$  was taken from the SAXS results,  $\rho_{PB}$  and  $\rho_m$  are calculated values.

contrast	diblock	matrix	$\rho_m$ ( $10^{10}$ cm <sup>-2</sup> )	$R_c$ (nm)	$\rho_c$ ( $10^{10}$ cm <sup>-2</sup> )	$\rho_{PB}$ ( $10^{10}$ cm <sup>-2</sup> )	$t_{PB}$ (nm)
(1)	PB2k-PEO5k	dPEO3k	6.0	8.2	$6.7 \pm 0.1$	0.4	$4.3 \pm 0.1$
(2)	PB2k-PEO5k	dPEO3k	6.0	8.2	6.7	0.4	4.3
	PB5k-PEO10k	dPEO10k	6.0	8.2	6.7	0.4	4.3
(3)	PB2k-PEO5k	D <sub>2</sub> O	6.3	8.2	6.7	0.4	4.3
(4)	PB2k-PEO5k	D <sub>2</sub> O	6.3	8.2	6.7	0.4	4.3

contrast	diblock	matrix	outer shell	$t_{PEO}$ (nm)	$\rho_{PEO}$ ( $10^{10}$ cm <sup>-2</sup> )	$N$	$l$ (nm)
(1)	PB2k-PEO5k	dPEO3k	dPEO	$1.1 \cdot 10^{-6} \pm 0.5$	6.0	$1.3 \pm 0.0$	0
(2)	PB2k-PEO5k	dPEO3k	hPEO	$4.5 \pm 0.1$	$3.3 \pm 0.2$	1.3	0
	PB5k-PEO10k	dPEO10k		$4.9 \pm 0.1$	$3.6 \pm 0.1$	$1.2 \pm 0.0$	0
(3)	PB2k-PEO5k	D <sub>2</sub> O	dPEO	$6.0 \pm 1.9$	$6.3 \pm 0.1$	1.3	0
(4)	PB2k-PEO5k	D <sub>2</sub> O	hPEO	$5.3 \pm 0.3$	$3.5 \pm 0.5$	1.3	0

The distance  $l$  between the particles in chain-like aggregates was fixed to zero as in contrast to SAXS, the polymer shell which determines this distance is now visible and this parameter does not play a role and can even be negative if polymer shells are overlapping.

### Calculation of volume fraction of PEO in shell from SANS

**Table 3S:** Calculated values of the volume fraction of PEO in the polymer shell from SANS analysis.

contrast	diblock	matrix	$t_{\text{PEO}}$ (nm)	$V_{\text{total}}$ (nm <sup>3</sup> )	$V_{\text{PEO shell}}$ (nm <sup>3</sup> )	$\rho_{\text{PEO}}$ (10 <sup>10</sup> cm <sup>-2</sup> )	$\phi_{\text{PEO}}$	$V_{\text{PEO}}$ (nm <sup>3</sup> )	$m_{\text{PEO}}$ (10 <sup>-21</sup> g)	$m_{\text{polymer}}$ (10 <sup>-21</sup> g)	$w_{\text{PEO}}$
(2)	PB2k-PEO5k	dPEO3k	4.5	20580	12398	3.4	0.49	5904	6744	12029	0.56
	PB5k-PEO10k	dPEO10k	4.9	22449	14268	3.5	0.44	6533	6714	11998	0.56
(4)	PB2k-PEO5k	D <sub>2</sub> O	5.3	18817	10635	3.5	0.33	5686	5686	10888	0.51

The mass fraction  $w_{\text{PEO}}$  was calculated using the obtained volume fractions of PEO in the outer shell to determine the volume of PEO. The volume for PB was calculated directly from the obtained shell thickness  $t_{\text{PB}}$ . Both volumes were transferred into the corresponding masses using densities of 0.9 g/cm<sup>3</sup> for PB and 1.1 g/cm<sup>3</sup> for PEO. The resulting values for  $w_{\text{PEO}}$  match very well to the prior result of 54.4% from elemental analysis.

### SAXS curves of aqueous samples

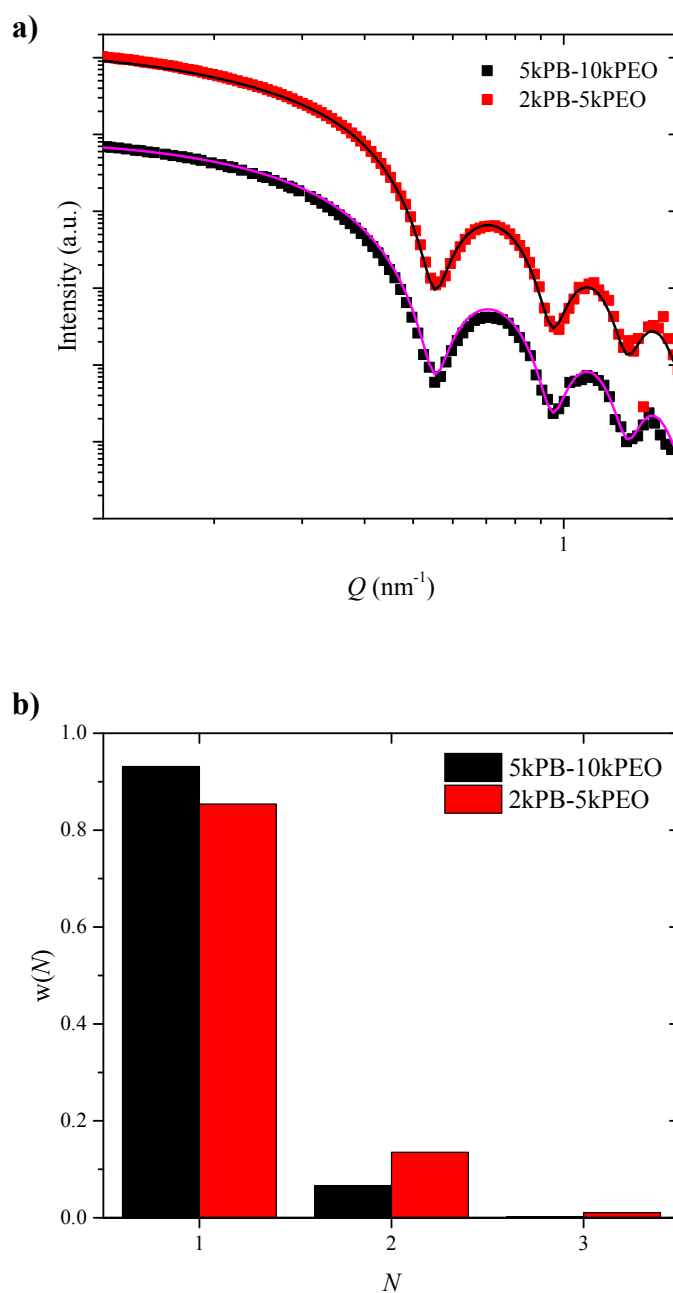
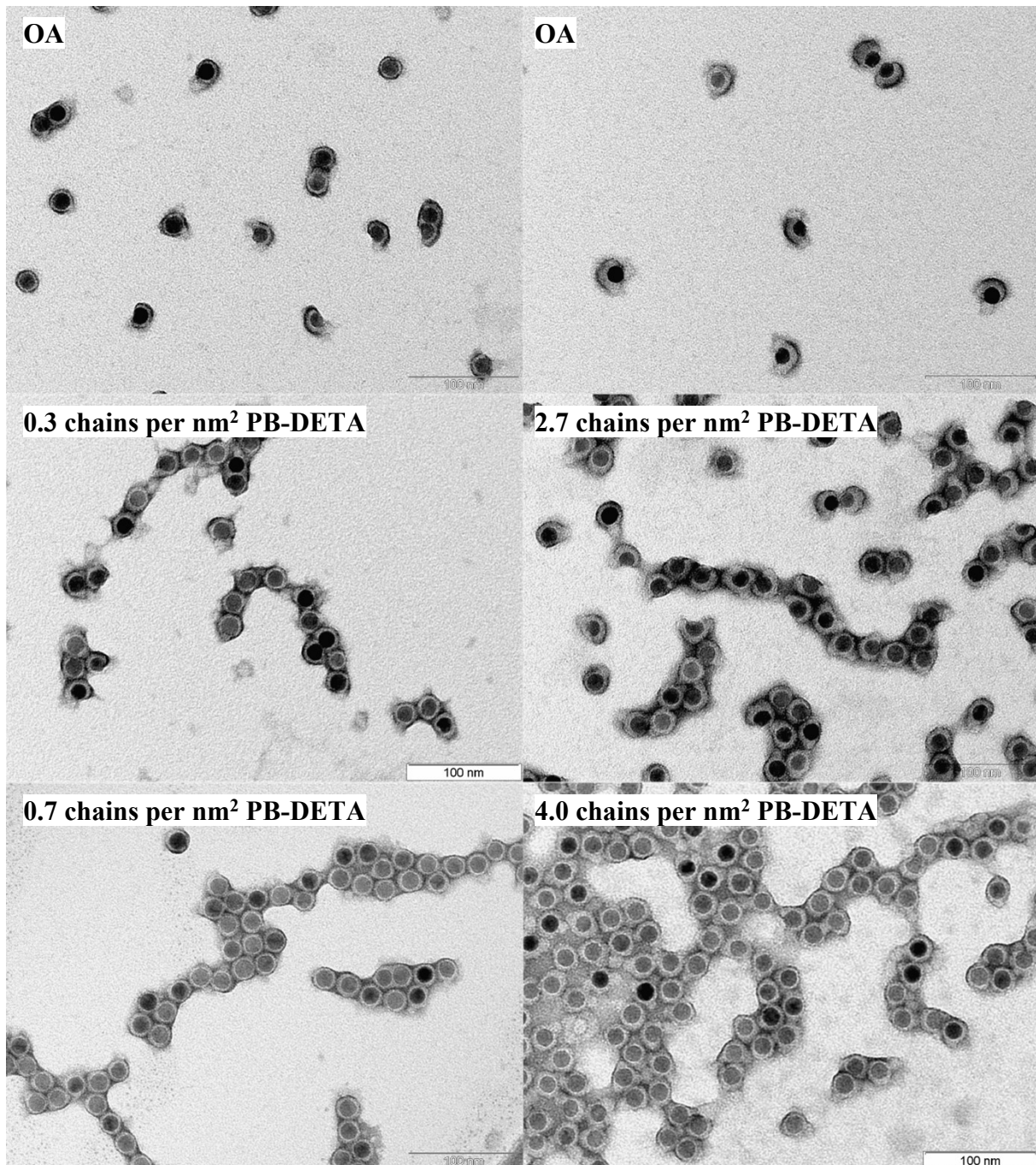


**Figure 5S:** (a) Experimental scattering curves (arbitrarily shifted) for 2kPB-5kPEO and 5kPB-10kPEO encapsulated SPIONs in water and (b) distribution for  $N$ .

**TEM of samples with different ligands and ligand excess**

2kPB-5kPEO

5kPB-10kPEO



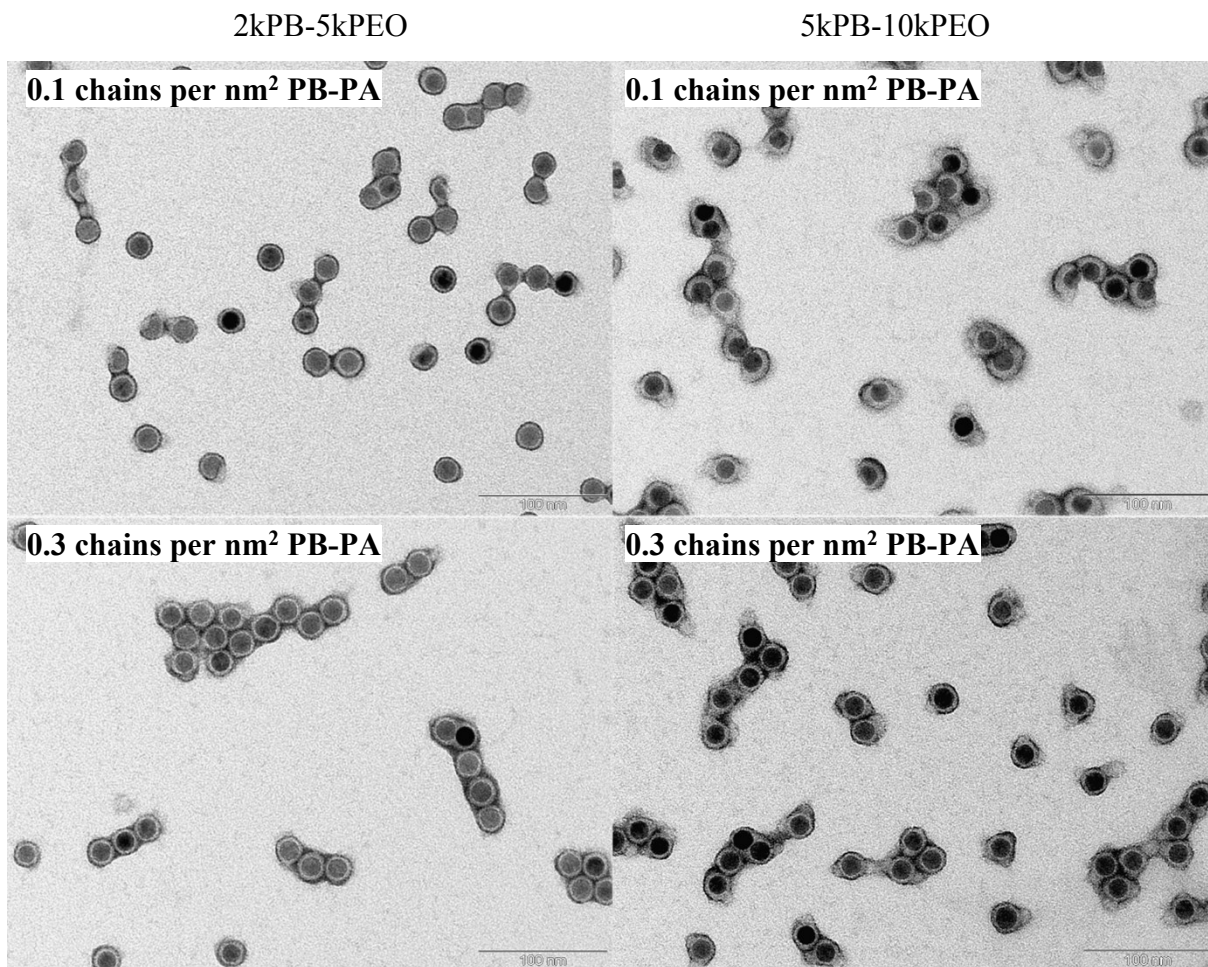


**Figure 6S:** TEM images of SPIONs, encapsulated with a 2kPB-5kPEO and 5kPB-10kPEO diblock copolymer, stabilized with different ligands and ligand excess.

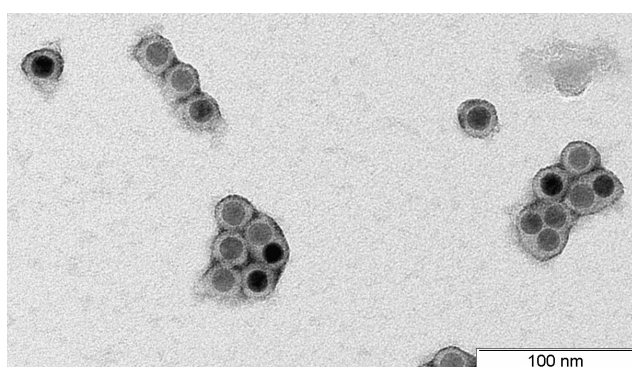


**Figure 7S:** TEM image of PB-*b*-PEO encapsulated SPIONs with a 5kPB-10kPEO polymer shell and a 5 kDa polymer ligand.

## SAXS of samples with different ligands and ligand excess

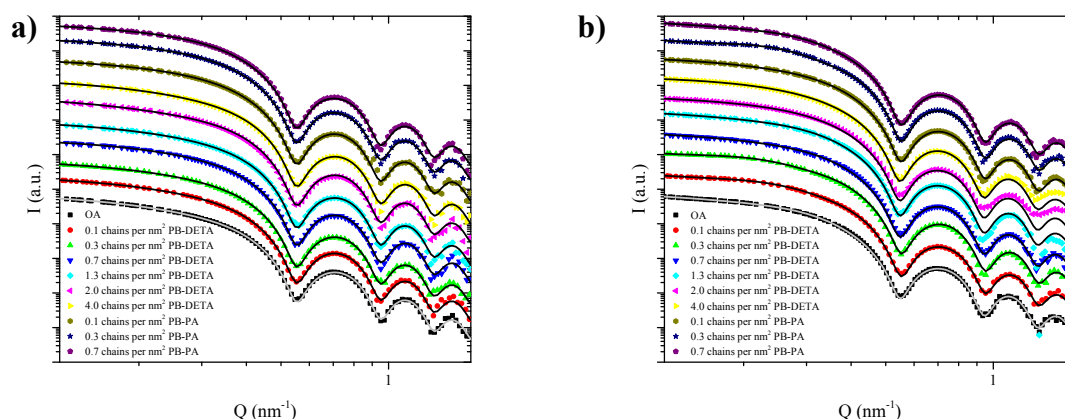


**Figure 8S:** Experimental scattering curves (arbitrarily shifted) for nanocomposites with 2kPB-5kPEO (a) and 5kPB-10kPEO (b) encapsulated SPIONs, stabilized with different ligands and ligand excess.

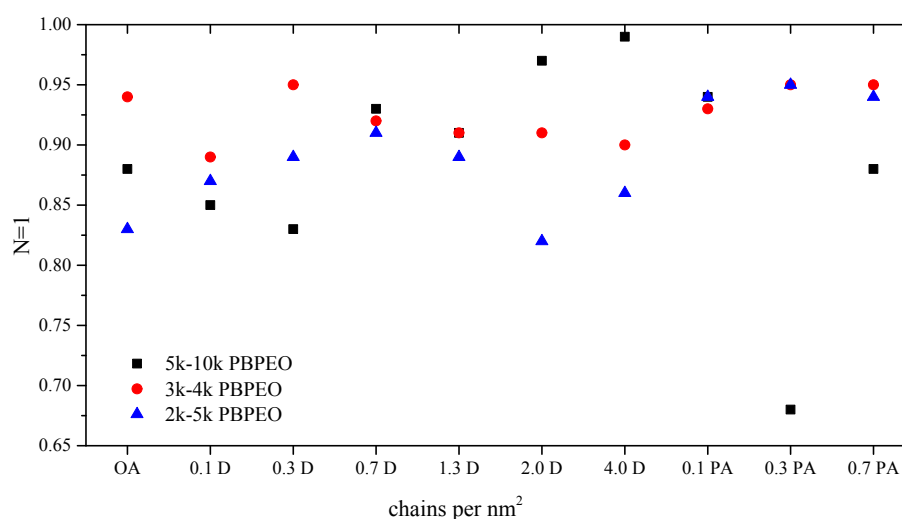


**Figure 9S:** Ratio of single NCs inside the nanocomposite for samples with different diblock copolymer sizes, different ligands and ligand excess.

## References

- 1 A. Feld, R. Koll, L. S. Fruhner, M. Krutyeva, W. Pyckhout-Hintzen, C. Weiß, H. Heller, A. Weimer, C. Schmidtke, M. S. Appavou, E. Kentzinger, J. Allgaier and H. Weller, *ACS Nano*, 2017, **11**, 3767–3775.
- 2 J. Köhler, H. Keul and M. Möller, *Chem. Commun.*, 2011, **47**, 8148–8150.
- 3 A. S. Sarac, *Prog. Polym. Sci.*, 1999, **24**, 1149–1204.
- 4 G. S. Hammond, J. N. Sen and C. E. Boozer, *J. Am. Soc.*, 1955, **77**, 3244–3248.

- 5 J. L. Faria and S. Steenken, *J. Chem. Soc., Perkin Trans. 2*, 1997, 1153–1159.
- 6 C. E. Hoyle, T. A. I. Y. Lee and T. Roper, *J. Polym. Sci. Part A Polym. Chem.*, 2004, **42**, 5301–5338.
- 7 K. Masaki, S. Ohkawara, T. Hirano, M. Seno and T. Sato, *J. Polym. Sci. Part A Polym. Chem.*, 2004, **42**, 4437–4447.
- 8 K. Hummel and G. Kaiser, *Kolloid-Zeitschrift und Zeitschrift für Polym.*, 1963, **197**, 90–97.
- 9 A. B. Lowe, *Polym. Chem.*, 2010, **17**, 17–36.